University Library

A gateway to Melbourne's research publications

Minerva Access is the Institutional Repository of The University of Melbourne

Author/s:
MANZIE, C;Zou, C;Nesic, D

Title:
Simplification Techniques for PDE Based Li-Ion Battery Models

Date:
2015-12-14

Citation:
MANZIE, C., Zou, C. & Nesic, D. (2015). Simplification Techniques for PDE Based Li-Ion Battery Models. 54th Annual Conference on Decision and Control (CDC), 54rd IEEE Conference on Decision and Control,CDC 2015, pp.3913-3921. IEEE. https://doi.org/10.1109/CDC.2015.7402828.

Persistent Link:
https://hdl.handle.net/11343/299361

Simplification techniques for PDE-based Li-Ion battery models

Chris Manzie, Changfu Zou, Dragan Nesic

***Abstract*— Battery systems are becoming increasingly prevalent as a source of power for applications across domains from consumer electronics to automotive, due to a range of factors such as portability and environmental considerations. The relatively high cost of batteries leads to a natural tradeoff in their use to ensure the lifetime of the battery is not unduly compromised while still delivering good performance.**

Similar tradeoffs have been successfully dealt with in other systems using model based control and estimation techniques, and this motivates their use for battery systems. Complicating this process is the complex nature of the physics-based models describing the operation of a battery cell, as these consist of a large number of partial differential equations spanning multiple, coupled domains.

This second paper of the tutorial session will briefly review the existing physics-based battery models, and introduce recent approaches that have been used to develop simplified models based on the original high-fidelity model. The assumptions underpinning the model simplification will be presented and discussed.

I. PDE MODEL EXTENSIONS

The complete one dimensional battery model encompasses several coupled domains. There are electrical, electrochemical, thermal and ageing dynamics each of which has been studied extensively, and often in isolation, by numerous researchers.

The high fidelity model introduced in [1] is extended in two ways for completeness of the model and to enable the different model simplification strategies introduced to be fully illustrated. The end point of the model simplification in this work is chosen to be the various single particle models available in the literature, although the specific model resulting from the simplification steps is naturally dependent on the number of assumptions applied during the model reductions. The efficacy of these assumptions is reliant on multiple factors, including the battery parameters but also the way in which the battery is used during charging and discharging.

In the first extension considered here, the electrical dynamics are included in preference to assuming outright they are negligible. This is as much for completeness of the starting point, as it is to demonstrate the model simplification methodology and requirements based around singular perturbation strategies for the battery model.

The second modification is based around the modelling of battery ageing. While capacity fade associated with active Li-ion loss in the positive electrode and solid-electrolyte-interface (SEI) film increase in the negative electrode is one common approach of quantifying battery ageing, it is typically modelled using a hybrid-domain approach whereby the level of degradation in the electrodes is kept constant through the charging process and adjusted *at the completion* of the charge cycle. This is modified here using a continuous time approach.

The full model used as the starting point is now described in the following sections.

A. Electrical dynamics

Previous cell models have typically neglected the dynamics of local potentials and currents in the solid particles and electrolyte, instead focusing on their steady-state behaviour. Here, for completeness and to help establish the first stages of the simplification methodology to be used, dynamics that explicitly describe the transient behaviour of the state variables of potentials of both the solid electrodes; potentials of the electrolyte in the two electrodes and separator; and finally current in the electrolyte in each of the three regions, thereby leading to seven dynamic equations.

To maintain a concise presentation from this point onwards, a shorthand notation is adopted where the superscripts $\pm$ represent either positive or negative electrode and j represents either of the electrodes or the separator, meaning the eight electrical dynamic equations are represented by the following three:

$$\epsilon_1 \frac{\partial \Phi_s^{\pm}(x,t)}{\partial t} = \frac{\partial \Phi_s^{\pm}(x,t)}{\partial x} + \frac{I(t) - i_e^{\pm}(x,t)}{\sigma^{\pm}}, \tag{1}$$

$$\epsilon_1 \frac{\partial \Phi_e^{j}(x,t)}{\partial t} = \frac{\partial \Phi_e^{j}(x,t)}{\partial x} + \frac{i_e^{j}(x,t)}{\kappa^{j}} - \frac{2R\gamma^j T^j(x,t)}{F} \frac{\partial \ln C_e^j(x,t)}{\partial x}, \tag{2}$$

$$\epsilon_1 \frac{\partial i_e^{\pm}(x,t)}{\partial t} = \frac{\partial i_e^{\pm}(x,t)}{\partial x} - F a^j J^{\pm}(x,t) \tag{3}$$

The parameters a and J in (1)-(3) are the specific interfacial area and total Li-ion flux at the surface of solid particles; σ, κ are the effective electronic and ionic conductivity; and R is the universal gas constant. The parameter ϵ_1 is a small positive constant inversely related to the transmission speeds of electric potential, ionic potential, and electrolyte current.

Algebraic equations are used to populate the dynamics in (1)-(3) starting with two constraint equations. The first applies to the on the current through solid i_s and electrolyte i_e phases, while the second links the total Li-ion flux to the normal intercalation flux, J_I and a side reaction flux, J_{sr}

This work was supported by the Australian Research Council through grant FT10100158

C. Manzie are Changfu Zou are with Department of Mechanical Engineering and Dragan Nesic is with the Department of Electrical Engineering, The University of Melbourne, Australia 3010 manziec@unimelb.edu.au

NOMENCLATURE

α_n, α_p	Anodic and cathodic charge transfer coefficients
α_{sr}	Charge transfer coefficient of side reaction
α_{sr}	Exchange current density of side reaction
δ_S	Entropy change
ϵ_1	Electrical time constant
η	Overpotential
η_{sr}	Overpotential of side reaction
γ	Transference number of the anion with respect to the solvent velocity
κ	Effective ionic conductivity
λ	Heat conductivity
μ_e	Volume fraction of electrolyte in the electrode
Φ_e^+, Φ_e^-	Electric potential in the electrolyte at the positive/negative electrodes
Φ_s^+, Φ_s^-	Electric potential in the solid particle at the positive/negative electrodes
ρ	Mass density
ρ_f	Average density of SEI film
σ	Effective electronic conductivity
σ_f	Conductivity of SEI film
A	Equivalent cross sectional area of the cell
a	Specific interfacial area at the surface of the solid particles
c	Specific heat
$C_{s\,\max}$	Maximum Li-ion concentration in solid particles
C_{ss}	Li Ion concentration at surface of solid particles
D_s^{eff}	Effective diffusion coefficient in solid particles
F	Faraday's constant
I	Applied current at terminal
i_e^+, i_e^-	Current in the electrolyte at the positive/negative terminals
i_s^+, i_s^-	Current in the solid particles at the positive/negative terminals
i_0	Exchange current density
J	Total Li-ion flux at the surface of the solid particles
J_I	Normal intercalation flux
J_{sr}	Side reaction flux
k	Reaction rate constant
L	Length of electrode in x-dimension
M_f	Average molecular weight of SEI film
R	Universal gas constant
r	Distance within spherical particle
R_f	SEI film resistance
SoC	State of charge
SoH	State of health
T	Temperature
U	Open circuit voltage
U_{sr}	Side reaction voltage
V	Terminal voltage
x	Distance along cell
$\bar{C}_{loss}$	Ion concentration lost
$\bar{C}_s$	Ion concentration in solid particles without loss
C_s	Ion concentration in solid particles with loss
Q_{max}	Maximum capacity
Q_{sr}	Capacity fade

indicative of battery ageing.

$$I(t) = i_s^{\pm}(x,t) + i_e^{\pm}(x,t) \tag{4}$$

$$J(x,t) = J_I^{\pm}(x,t) + J_{sr}^{\pm}(x,t) \tag{5}$$

By denoting k the reaction rate constant; α_n, α_p the anodic and cathodic charge-transfer coefficients of the main intercalation reaction; $C_{s\max}$ the maximum possible Li-ion concentration in the solid particles; R_p the radius of the solid particles; and C_{ss} is the Li-ion concentration at the surface of these particles, *i.e.*

$$C_{ss}^{\pm}(x,t) := C_s^{\pm}(x, r = R_p, t). \tag{6}$$

The exchange current density, i_0, and the overpotential, η, in each electrode are given by:

$$i_0^{\pm}(x,t) = k^{\pm} C_e^{\pm}(x,t)^{\alpha_n} (C_{s\max}^{\pm} - C_{ss}^{\pm}(x,t))^{\alpha_n} C_{ss}^{\pm}(x,t)^{\alpha_p} \tag{7}$$

$$\eta^{\pm}(x,t) = \Phi_s^{\pm}(x,t) - \Phi_e^{\pm}(x,t) - U^{\pm}(x,t) - F R_f(x,t) J^{\pm}(x,t) \tag{8}$$

Finally the intercalation flux from (5) may be represented in terms of these defined variables by the algebraic equation

$$J_I^{\pm}(x,t) = \frac{i_0^{\pm}(x,t)}{F} \left(e^{\frac{\alpha_n F \eta^{\pm}(x,t)}{RT^{\pm}(x,t)}} - e^{-\frac{\alpha_p F \eta^{\pm}(x,t)}{RT^{\pm}(x,t)}} \right). \tag{9}$$

B. Electrochemical dynamics

In the absence of battery ageing, the diffusion equation for ion concentrations in the solid particles is represented by

$$\frac{\partial \bar{C}_s^{\pm}(x,r,t)}{\partial t} = \frac{D_s^{\text{eff},\pm}}{r^2} \frac{\partial}{\partial r} \left(r^2 \frac{\partial \bar{C}_s^{\pm}(x,r,t)}{\partial r} \right), \tag{10}$$

where D_s^{eff} represents the effective diffusion coefficient in the solid particles.

To reflect the degradation of the battery capacity , Q_{sr}, caused by the accumulated effect of a side reaction in the positive electrode only, the total ion concentration lost is modelled as the following relationship when $Q_{\max}$ is the maximum nominal capacity of a battery:

$$C_{\text{loss}}^{+}(x,r,t) = \frac{Q_{sr}(x,t)}{Q_{\max}} \bar{C}_s^{+}(x,r,t), \tag{11}$$

Consequently, the dynamic equation describing the remaining concentration of ions at the positive electrode, C_s^+, follows from conservation constraint and satisfies

$$\frac{\partial C_s^{+}(x,r,t)}{\partial t} = \frac{\partial \bar{C}_s^{+}(x,r,t)}{\partial t} - \frac{Q_{sr}(x,t)}{Q_{\max}} \frac{\partial \bar{C}_s^{+}(x,r,t)}{\partial t} - \frac{\bar{C}_s^{+}(x,r,t)}{Q_{\max}} \frac{\partial Q_{sr}(x,t)}{\partial t}, \tag{12}$$

Inside the negative electrode, the active Li-ion loss is typically ignored [2], [3], allowing the dynamic behaviour of Li-ion concentration to be given completely by (10), i.e.

$$\frac{\partial C_s^{-}(x,r,t)}{\partial t} = \frac{D_s^{\text{eff},-}}{r^2} \frac{\partial}{\partial r} \left(r^2 \frac{\partial C_s^{-}(x,r,t)}{\partial r} \right). \tag{13}$$

In the electrolyte of the electrodes and separator, the change of Li-ion concentration is related to its gradient-induced diffusive flow and the local electrolyte current and is governed by [4], [1]

$$\frac{\partial C_e^j(x,t)}{\partial t} = \frac{D_e^{\text{eff},j}}{\mu_e^j} \frac{\partial}{\partial x} \left(\frac{\partial C_e^j(x,t)}{\partial x} \right) + \frac{\gamma^j}{F \mu_e^j} \frac{\partial i_e^j}{\partial x}, \tag{14}$$

C. Thermal dynamics

The heat sources inside a cell include the reaction heat generation, reversible heat generation, and ohmic heat generation. The generated heat is transported through the battery internal conductivity and convection between battery surface and the surrounding environment. To capture temperature distribution and evolution in a Li-ion battery cell, the thermal balance equation is provided as [5]

$$\begin{aligned}\rho^j c^j \frac{\partial T^j(x,t)}{\partial t} =& \lambda^j \frac{\partial^2 T^j(x,t)}{\partial x^2} - (I(t) - i_e^j(x,t)) \frac{\partial \Phi_s^j(x,t)}{\partial x} \\ & - i_e^j(x,t) \frac{\partial \Phi_e^j(x,t)}{\partial x} + F a^j J^j(x,t)\, \eta^j(x,t) \\ & + F a^j J^j(x,t)\, T^j(x,t) \delta_S^j, \end{aligned} \tag{15}$$

where δ_S is the entropy change, and ρ, c, λ are the mass density, specific heat, and heat conductivity.

On the right-hand side of (15), the second and third terms represent the reaction heat, and the last two terms are separately the ohmic heat and reversible heat. From the above equation, it follows that the electrical states, Φ_s, Φ_e, i_e, are directly involved in heat generation. The elevated temperature in turn affects the main intercalation reaction through (2) and accelerates the dynamics of battery ageing via (18).

D. Ageing dynamics

While there are many complex mechanisms associated with battery ageing and degradation, the underlying effect is a loss in ion concentration at the positive electrode, as given by (11). The model adopted here is the lost ions contribute to the growth of a resistive and insoluble SEI film at the negative electrode as in [2], [3]. As battery operating cycles increase, the film grows and leads to both capacity fade and a rise in the internal resistance.

A lumped capacity fade has been formulated in the initial State of Health (SoH) model of [2]. However, physically, the side reaction as well as its resulting parasitic flux and SEI film may exhibit strong spatial variations. To model this process, a spatially distributed aged capacity, $Q_{sr}(x,t)$, is proposed here and introduced in the dynamic equations of capacity fade and internal resistance as:

$$\frac{\partial Q_{sr}(x,t)}{\partial t} = -F a^- A^- L^- J_{sr}(x,t), \tag{16}$$

$$\frac{\partial R_f(x,t)}{\partial t} = -\frac{M_f}{\rho_f \sigma_f} J_{sr}(x,t), \tag{17}$$

where σ_f, M_f, ρ_f are respectively the conductivity, average molecular weight, and average density of the constituent compounds of the SEI film; and A is the equivalent cross-sectional area along x direction of the electrode. Note: L^j represents the length of the electrode and separator, and $L := L^+ + L^- + L^{sep}$ is the total length of the battery cell.

In (16)-(17), by assuming the side reaction to be irreversible, the side reaction flux J_{sr} can be modelled by Tafel equation [2], [6]

$$J_{sr}(x,t) = \frac{-i_{0sr}}{F} e^{\frac{-F\alpha_{sr}\eta_{sr}(x,t)}{RT^-(x,t)}}, \tag{18}$$

where $\alpha_{sr}, \eta_{sr}, i_{0sr}$ are the charge-transfer coefficient, overpotential, and exchange current density of the side reaction, respectively. The overpotential that determines the rate of side reaction is provided by

$$\eta_{sr}(x,t) = \Phi_s^-(x,t) - \Phi_e^-(x,t) - U_{sr} - F R_f(x,t) J^-(x,t).$$

E. Complete integrated cell model

With the dynamic equations describing each domain now described, scalar quantities used as the outputs of the cell can be defined. The terminal voltage, $V(t)$ is presented as the difference between the positive and negative electrical potentials at the terminals, and is the only directly measurable output.

$$V(t) = \Phi_s^+(L,t) - \Phi_s^-(0,t), \tag{19}$$

The scalar quantities defined as State of Health (SoH) and State of Charge (SoC), while not directly measurable, are typically used to quantify the state of the battery in a concise manner. The SOC in each electrode is defined as the ratio between the averaged available Li-ion concentration and maximum possible concentration [1],

$$SOC^{\pm}(t) = \frac{3}{L^{\pm} R_p^{3,\pm}} \int_0^{L^{\pm}} \int_0^{R_p^{\pm}} \frac{C_s^{\pm}(x,r,t)}{C_{\mathrm{smax}}^{\pm}} dr dx, \tag{20}$$

SoH represents the spatially averaged capacity fade due to the side reaction in the anode electrode, and normalised relative to the initial maximum available capacity [7]. As discussed in Section I-D, no degradation is assumed to take place in the cathode.

$$SOH(t) = 1 - \int_0^{L^-} \frac{Q_{sr}(x,t)}{Q_{\max}} dx. \tag{21}$$

Coupled with boundary conditions that maintain continuity across the interface boundaries, the entire system of 17 PDEs and associated algebraic equations may be represented in block diagram form as illustrated in Figure 1. This highlights the coupling between the domains in the system equations and helps to motivate the approach of the following sections.

II. Model representation in Hilbert space

While a complete dynamic cell model has now been described across equations (1)-(21), it is not immediately obvious where model simplification should begin. To facilitate a structured and systematic approach to the model simplification, it is helpful to abstract away some of the specific detail. In doing so, the first step is to introduce the system input defined as $u := I(t)$ and the 17th order state vector, $\bar{\mathbf{x}}$:

$$\bar{\mathbf{x}}^- := \left[C_s^-, C_e^-, \Phi_s^-, \Phi_e^-, i_e^-, T^-, Q_{sr}, R_f\right]^T \tag{22}$$

$$\bar{\mathbf{x}}^{sep} := \left[C_e^{sep}, \Phi_e^{sep}, T^{sep}\right]^T \tag{23}$$

$$\bar{\mathbf{x}}^+ := \left[C_s^+, C_e^+, \Phi_s^+, \Phi_e^+, i_e^+, T^+\right]^T \tag{24}$$

$$\bar{\mathbf{x}} := \left[\bar{\mathbf{x}}^-, \bar{\mathbf{x}}^+, \bar{\mathbf{x}}^{sep}\right]^T \tag{25}$$

Meanwhile the measurable and unmeasurable outputs may be denoted $\mathbf{y}_c = [SOC^-(t), SOC^+(t), SOH(t)]^T := g(\bar{\mathbf{x}})$, and $\mathbf{y}_m = V(t) := q(\bar{\mathbf{x}})$.

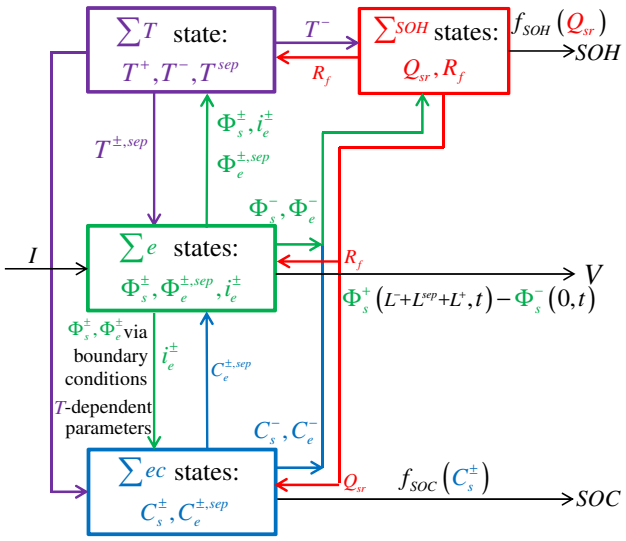

Fig. 1. Full model

The domain of definition for all the state variables is $\mathcal{D}(x,r) = \{(x,r)|x \in [0,L], r \in [0,R_p]\}$. With the states within $\mathcal{D}(x,r)$, we now introduce the following matrices, :

$$H^- = \begin{pmatrix} 0 \\ 0 \\ (I - i_e^-)(\epsilon_{\Phi s}\sigma^{\text{eff},-})^{-1} \\ i_e^-(\epsilon_{\Phi e}\kappa^{\text{eff},-})^{-1} \\ Fa^- J^- \epsilon_{ie}^{-1} \\ Fa^- J^-(\eta^- + T^-\delta_S^-)(\rho^- c^-)^{-1} \\ -Fa^- A^- L^- J_{sr} \\ -M_f J_{sr}(\rho_f \sigma_f)^{-1} \end{pmatrix}$$

$$H^{sep} = \begin{pmatrix} 0 \\ -\frac{i^{sep}}{\kappa^{sep}\epsilon_{\Phi e}} \\ \frac{Fa^{sep} J^{sep}(\eta^{sep} + T^{sep}\delta_S^{sep})}{\rho^{sep} c^{sep}} \end{pmatrix}$$

$$H^+ = \begin{pmatrix} -Fa^- A^- L^- J_{sr} C_s^+ Q_{\max}^{-1} \\ 0 \\ (I - i_e^+)(\epsilon_{\Phi s}\sigma^{\text{eff},+})^{-1} \\ i_e^+(\epsilon_{\Phi e}\kappa^{\text{eff},+})^{-1} \\ Fa^+ J^+ \epsilon_{ie}^{-1} \\ Fa^+ J^+(\eta^+ + T^+\delta_S^+)(\rho^+ c^+)^{-1} \end{pmatrix}$$

$$H(\bar{\mathbf{x}}, u) = \text{diag}(H^-, H^{sep}, H^+)$$

And,

$$S_1^- = \begin{pmatrix} 0 & 0 & 0 & 0 & 0 & 0 & 0 & 0 \\ 0 & 0 & 0 & 0 & \frac{\gamma^-}{F\mu_e^-} & 0 & 0 & 0 \\ 0 & 0 & \frac{1}{\epsilon_{\Phi s}} & 0 & 0 & 0 & 0 & 0 \\ 0 & \frac{-2R\gamma^- T^-}{F\epsilon_{\Phi s} C_e^-} & 0 & \frac{1}{\epsilon_{\Phi e}} & 0 & 0 & 0 & 0 \\ 0 & 0 & 0 & 0 & \frac{1}{\epsilon_{ie}} & 0 & 0 & 0 \\ 0 & 0 & -I + i_e^- & -i_e^- & 0 & 0 & 0 & 0 \\ 0 & 0 & 0 & 0 & 0 & 0 & 0 & 0 \\ 0 & 0 & 0 & 0 & 0 & 0 & 0 & 0 \end{pmatrix}$$

$$S_1^{sep} = \begin{pmatrix} 0 & 0 & 0 \\ -\frac{2R\gamma^{sep} T^{sep}}{F C_e^{sep}} & \frac{1}{\epsilon_{\Phi e}} & 0 \\ 0 & -I & 0 \end{pmatrix}$$

$$S_1^+ = \begin{pmatrix} 0 & 0 & 0 & 0 & 0 & 0 & 0 & 0 \\ 0 & 0 & 0 & 0 & \frac{\gamma^+}{F\mu_e^+} & 0 & 0 & 0 \\ 0 & 0 & \frac{1}{\epsilon_{\Phi s}} & 0 & 0 & 0 & 0 & 0 \\ 0 & \frac{-2R\gamma^+ T^+}{F\epsilon_{\Phi s} C_e^+} & 0 & \frac{1}{\epsilon_{\Phi e}} & 0 & 0 & 0 & 0 \\ 0 & 0 & 0 & 0 & \frac{1}{\epsilon_{ie}} & 0 & 0 & 0 \\ 0 & 0 & \frac{-I + i_e^+}{\rho^+ c^+} & \frac{-i_e^+}{\rho^+ c^+} & 0 & 0 & 0 & 0 \end{pmatrix}$$

$$S_1 = \text{diag}(S_1^-, S_1^{sep}, S_1^+)$$

Similarly,

$$\begin{aligned}
F_1^- &= \text{diag}(2D_s^{\text{eff},-}/r, 0, 0, 0, 0, 0, 0, 0), \\
F_1^{sep} &= F_2^{sep} = \text{zeros}(3,3), \\
F_1^+ &= \text{diag}(2D_s^{\text{eff},+}(1 - Q_{sr}/Q_{\max}), 0, 0, 0, 0, 0), \\
F_1 &= \text{diag}(F_1^-, F_1^{sep}, F_1^+) \\
F_2^- &= \text{diag}(D_s^{\text{eff},-}, 0, 0, 0, 0, 0, 0, 0), \\
F_2^+ &= \text{diag}(D_s^{\text{eff},+}(1 - Q_{sr}/Q_{\max}), 0, 0, 0, 0, 0), \\
F_2 &= \text{diag}(F_2^-, F_2^{sep}, F_2^+) \\
S_2^- &= \text{diag}(0, D_e^{\text{eff},-}/\mu_e^-, 0, 0, 0, \lambda^-/(\rho^- c^-), 0, 0), \\
S_2^{sep} &= \text{diag}(D_e^{\text{eff},sep}/\mu_e^{sep}, 0, \lambda^{sep}/(\rho^{sep} c^{sep})), \\
S_2^+ &= \text{diag}(0, D_e^{\text{eff},+}/\mu_e^+, 0, 0, 0, \lambda^+/(\rho^+ c^+)), \\
S_2 &= \text{diag}(S_2^-, S_2^{sep}, S_2^+)
\end{aligned}$$

Subsequently, the complete cell model given in the previous section can be written in the compact notation:

$$\begin{aligned}
\frac{\partial \bar{\mathbf{x}}}{\partial t} &= F_1 \frac{\partial \bar{\mathbf{x}}}{\partial r} + S_1 \frac{\partial \bar{\mathbf{x}}}{\partial x} + F_2 \frac{\partial^2 \bar{\mathbf{x}}}{\partial r^2} \\
&\quad + S_2 \frac{\partial^2 \bar{\mathbf{x}}}{\partial x^2} + H(\bar{\mathbf{x}}, u), \qquad (26) \\
\mathbf{y}_c &= g(\bar{\mathbf{x}}), \qquad (27) \\
\mathbf{y}_m &= q(\bar{\mathbf{x}}), \qquad (28)
\end{aligned}$$

subject to appropriate boundary conditions on the states at the interfaces between each of the electrodes and the separator.

To present the PDE system precisely and also simplify the notation, the infinite dimensional system (26)-(28) is reformulated within the Hilbert space $\mathscr{H}(\mathcal{D}, \mathbb{R}^n)$. Define the state function $\mathbf{x}$ on $\mathscr{H}$ as:

$$\mathbf{x}(t) = \bar{\mathbf{x}}(x,r,t),\ \forall t > 0, \forall (x,r) \in \mathcal{D}(x,r),$$

the operator $\mathcal{F}$ in $\mathscr{H}(\mathcal{D}, \mathbb{R}^n)$ as:

$$\begin{aligned}
\mathcal{F}\mathbf{x} &= F_1 \frac{\partial \bar{\mathbf{x}}}{\partial r} + S_1 \frac{\partial \bar{\mathbf{x}}}{\partial x} + F_2 \frac{\partial^2 \bar{\mathbf{x}}}{\partial r^2} + S_2 \frac{\partial^2 \bar{\mathbf{x}}}{\partial x^2}, \\
\mathbf{x} &\in D(\mathcal{F}) = \{\mathbf{x} \in \mathscr{H}(\mathcal{D}, \mathbb{R}^n);\ \text{Boundary conds.}\},
\end{aligned}$$

and the output operators as:

$$\mathcal{G}\mathbf{x} = g, \quad \mathcal{Q}\mathbf{x} = q.$$

Then, the battery system dynamics may be represented compactly in the form given below (and henceforth denoted

as Σ^1):

$$\dot{\mathbf{x}} = \mathcal{F}\mathbf{x} + H(\mathbf{x}, u),\ \ \mathbf{x}(0) = \mathbf{x}_0, \tag{29}$$

$$\mathbf{y}_c = \mathcal{G}\mathbf{x}, \tag{30}$$

$$\mathbf{y}_m = \mathcal{Q}\mathbf{x}, \tag{31}$$

where $H(\mathbf{x}(t), u(t))$=$H(\bar{\mathbf{x}}(x, r, t), u(t))$ and $\mathbf{x}_0$=$\bar{\mathbf{x}}_0$.

The principle reason for reformulating the model in Hilbert space is to expose the natural singular perturbation style that exists, and to therefore consider the use of time scale separation ideas in model simplification. This is complicated by the lack of formal results for the use of singular perturbation techniques with systems of PDEs, however it is not without precedent - for example [8] use singular perturbation techniques for model simplification of several PDE-based processes, albeit with a different underlying structure to those encountered in modelling a battery cell.

III. PDE SIMPLIFICATION THROUGH SINGULAR PERTURBATION TECHNIQUES

This section takes the Hilbert space representation, Σ^1, defined in the the previous section and introduces assumptions under which model simplications in Hilbert space reminiscent of the singular perturbation approaches of [9], [10] for ordinary differential equations might be applicable.

A. Model Simplification Step 1: Models Σ_f^2 & Σ_s^2

To investigate the time scale separation, the Σ_1-system can be rewritten in the standard form of singularly perturbed systems

$$\dot{\mathbf{x}}_s = \mathcal{F}_s\mathbf{x}_s + H_s(\mathbf{x}_s, \mathbf{x}_f, u), \mathbf{x}_s(0) = \mathbf{x}_{s0}, \tag{32}$$

$$\epsilon_1\dot{\mathbf{x}}_f = \mathcal{F}_f\mathbf{x}_f + H_f(\mathbf{x}_s, \mathbf{x}_f, u), \mathbf{x}_f(0) = \mathbf{x}_{f0}, \tag{33}$$

$$\mathbf{y}_c = \mathcal{G}[\mathbf{x}_s, \mathbf{x}_f]^T \tag{34}$$

$$\mathbf{y}_m = \mathcal{Q}[\mathbf{x}_s, \mathbf{x}_f]^T, \tag{35}$$

where in the negative electrode, the state function $\mathbf{x}$ can be expressed more explicitly to include $\mathbf{x}_s^- := [C_s^-, C_e^-, T^-, Q_{sr}, R_f]^T$ and $\mathbf{x}_f^- := [\Phi_s^-, \Phi_e^-, i_e^-]^T$. Similar cases can be done for the positive electrode and separator. The functions H_s, H_f are continuous and bounded in their arguments for $(\mathbf{x}_s, \mathbf{x}_f, u) \in \mathscr{H}_s \times \mathscr{H}_f \times \mathbb{U}$, where $\mathscr{H}_s$ and $\mathscr{H}_f$ are subspaces of $\mathscr{H}$.

The following two Assumptions are now made about the model.

Assumption 1: $\epsilon_1 << 1$

Assumption 2: $|\dot{u}(t)| << 1/\epsilon_1$ for almost all t.

In essence, these Assumptions are *implicitly* assumed in prior battery modelling work and reflect the natural time scales present in the system - i.e. the electrical dynamics are significantly faster than all others present (Assumption 1) and the system input is not changing at the same rate as these electrical dynamics (Assumption 2). The latter assumption is necessary for decoupling of the equations and consistent with requirements for a similarly structured system of ordinary differential equations.

Continuing with the analogy with systems of ODEs, under Assumptions 1 and 2 it appears sensible to decouple the system into boundary layer and reduced systems. For approximation of the slow states, the fast dynamic states may be replaced by the solution to

$$0 = \mathcal{F}_f\mathbf{x}_f + H_f(\mathbf{x}_s, \mathbf{x}_f, u) \tag{36}$$

The real root of (36) is known to exist in the arguments $\forall t > 0$ and $\forall (x, r) \in \mathcal{D}(x, r)$ and may be defined as $\mathbf{x}_f^* := h(\mathbf{x}_s, u)$. This leads to the reduced system representation for the "slow" states of Σ^1, denoted as Σ_s^2, given by:

$$\dot{\mathbf{x}}_s = \mathcal{F}_s\mathbf{x}_s + H_s(\mathbf{x}_s, h(\mathbf{x}_s, u), u), \mathbf{x}_s(0) = \mathbf{x}_{s0}, \tag{37}$$

$$\mathbf{y}_c = \mathcal{G}[\mathbf{x}_s, h(\mathbf{x}_s, u)]^T, \tag{38}$$

$$\mathbf{y}_m = \mathcal{Q}[\mathbf{x}_s, h(\mathbf{x}_s, u)]^T, \tag{39}$$

For completeness, and in keeping with the singular perturbation analogy, the fast state dynamics of Σ^1 could be approximated by keeping the slow states and input constant thereby resulting in the boundary layer (fast) system, Σ_f^2:

$$\frac{d\mathbf{x}_f}{d\tau} = \mathcal{F}_f\mathbf{x}_f + H_f(\mathbf{x}_{s0}, \mathbf{x}_f, u_0),\ \mathbf{x}_f(0) = \mathbf{x}_{f0}. \tag{40}$$

To shift the quasi-steady state of $\mathbf{x}_f$ to the origin, define $\mathbf{z}_f := \mathbf{x}_f - h(\mathbf{x}_{s0}, u_0)$ so (40) can be reformulated as

$$\frac{d\mathbf{z}_f}{d\tau} = \mathcal{F}_f(\mathbf{z}_f + h(\mathbf{x}_{s0}, u_0)) + H_f(\mathbf{x}_{s0}, \mathbf{z}_f + h(\mathbf{x}_{s0}, u_0), u_0). \tag{41}$$

Assumption 3: The boundary layer battery system given in (41) is uniformly globally exponentially stable (UGES).

This Assumption is readily validated numerically, and is used here to ensure the boundary layer system has a similar structure to that required in classical singular perturbation theory. For systems of ODEs such as those covered by Tikhonov, satisfaction of this Assumption ensures the trajectories of the fast state variables converge to the quasi-steady states of (36).

Up to this point in the model simplification, the typical battery model has been recovered, and the results are perhaps unsurprising. However, having recaptured the expected result using an adaption of singular perturbation techniques, there is some degree of confidence in reapplying it for further model reduction. Consequently, we now continue to apply the singular perturbation philosophy to the non-electrical dynamics remaining in the model Σ_s^2.

B. Model Simplification Step 2: Models Σ_m^3 & Σ_s^3

The model of the slower dynamics following the first simplification step, Σ_s^2 is now considered in isolation for further model simplification. Intuitively, one might reasonably expect that the dynamics associated with cell degradation are significantly slower than the other cell dynamics, and this serves as a motivating factor in the next model decomposition. By defining i_o^* as a representative value of i_o and explicitly exposing the non-dimensional parameter $\frac{i_{0sr}}{i_o^*}$

dependence in Σ_s^2, the system of (35) may be rewritten as:

$$\begin{aligned}
\dot{\mathbf{x}}_{s'} &= \tfrac{i_{0sr}}{i_o^*}\mathcal{F}_{s'}\mathbf{x}_{s'} + \tfrac{i_{0sr}}{i_o^*}H_{s'}(\mathbf{x}_{s'},\mathbf{x}_m,h(\mathbf{x}_{s'},\mathbf{x}_m,u),u),\\
\mathbf{x}_{s'}(0) &= \mathbf{x}_{s'0},\\
\dot{\mathbf{x}}_m &= \mathcal{F}_m\mathbf{x}_m + H_m(\mathbf{x}_{s'},\mathbf{x}_m,h(\mathbf{x}_{s'},\mathbf{x}_m,u),u),\\
\mathbf{x}_m(0) &= \mathbf{x}_{m0},\\
\mathbf{y}_c &= \mathcal{G}[\mathbf{x}_{s'},\mathbf{x}_m,h(\mathbf{x}_{s'},\mathbf{x}_m,u)]^T,\\
\mathbf{y}_m &= \mathcal{Q}[\mathbf{x}_{s'},\mathbf{x}_m,h(\mathbf{x}_{s'},\mathbf{x}_m,u)]^T,
\end{aligned} \tag{42}$$

where the state functions $\mathbf{x}_{s'}{:=}[C_{s,s}, Q_{sr}, R_f]^T$ and $\mathbf{x}_m{:=}[C_{s,m}, C_e, T]^T$. Within this set of equations, the solid-phase Li-ion concentration, C_s, is couples the normal diffusion and SEI film growth dynamics, and thus it may be represented as two states after decomposition, $C_{s,m}$ and $C_{s,s}$. Note that the functions $H_{s'}, H_m$ are continuous and bounded in their arguments for $(\mathbf{x}_{s'},\mathbf{x}_m,u){\in}\mathscr{H}_{s'}{\times}\mathscr{H}_m{\times}\mathbb{U}$ and $\mathscr{H}_{s'}$,$\mathscr{H}_m{\subset}\mathscr{H}$.

The following assumption is now introduced.

Assumption 4: The non-dimensional parameter $\frac{i_{0sr}}{{i_o}^*} \ll 1$.

Assumption 4 may be justified intuitively by considering that during the charge and discharge process, the electrochemical and thermal states in a battery cell have significant change within a couple of minutes or hours. By comparison, the degree of battery degradation parameterised by i_{0sr} is several orders of magnitude slower than the normal intercalation reaction. Furthermore, previous studies have shown i_{0sr} is a positive parameter on the order of $1e{-}6$, in contrast the value of i_0 is as large as 1 [2].

With a time scale separation structure identified for Σ_s^2, under Assumption 4 the boundary layer and reduced systems can again be identified using a singular perturbation approach, leading to the following boundary layer system Σ_m^3, which corresponds to the medium time scale of the original Σ^1 model:

$$\begin{aligned}
&\dot{\mathbf{x}}_{s'} = 0,\ \ \mathbf{x}_{s'}(0) = \mathbf{x}_{s'0},\\
&\dot{\mathbf{x}}_m = \mathcal{F}_m\mathbf{x}_m + H_m(\mathbf{x}_{s'},\mathbf{x}_m,h(\mathbf{x}_{s'},\mathbf{x}_m,u),u),\\
&\mathbf{x}_m(0) = \mathbf{x}_{m0},\\
&\mathbf{y}_c = \mathcal{G}[\mathbf{x}_{s'},\mathbf{x}_m,h(\mathbf{x}_{s'},\mathbf{x}_m,u)]^T,\\
&\mathbf{y}_m = \mathcal{Q}[\mathbf{x}_{s'},\mathbf{x}_m,h(\mathbf{x}_{s'},\mathbf{x}_m,u)]^T,
\end{aligned} \tag{43}$$

In (43), the differential equations in terms of $\mathbf{x}_{s'}$ from (42) are approximated by an algebraic equation through which the slow time scale state $\mathbf{x}_{s'}$ is fixed to be a constant, *i.e.* $\mathbf{x}_{s'0}$. After elimination of the dynamics of $\mathbf{x}_{s'}$, the state $\mathbf{x}_m$ is decoupled from the full-order battery system.

To remove the abstraction of the Hilbert space representations, the medium time scale battery model, Σ_m^3, following the use of singular perturbation steps can now be expressed in terms of the original (physical) states as:

$$\begin{aligned}
\frac{\partial C_{s,m}^+(x,r,t)}{\partial t} &= \frac{D_s^{\text{eff},+}}{r^2}\frac{\partial}{\partial r}\left(r^2\frac{\partial C_{s,m}^+(x,r,t)}{\partial r}\right),\\
\frac{\partial C_s^-(x,r,t)}{\partial t} &= \frac{D_s^{\text{eff},-}}{r^2}\frac{\partial}{\partial r}\left(r^2\frac{\partial C_s^-(x,r,t)}{\partial r}\right),\\
\frac{\partial C_e^j(x,t)}{\partial t} &= \frac{\partial}{\partial x}\left(\frac{D_e^{\text{eff},j}}{\mu_e^j}\frac{\partial C_e^j(x,t)}{\partial x}\right) + \frac{\gamma^j}{F\mu_e^j}\frac{\partial i_e^j}{\partial x},\\
\rho^j c^j\frac{\partial T^j(x,t)}{\partial t} &= \lambda^j\frac{\partial^2 T^j(x,t)}{\partial x^2} - (I(t) - i_e^j(x,t))\frac{\partial \Phi_s^j(x,t)}{\partial x}\\
&\quad - i_e^j(x,t)\frac{\partial \Phi_e^j(x,t)}{\partial x} + Fa^jJ_I^j(x,t)\,\eta^j(x,t)\\
&\quad + Fa^jJ_I^j(x,t)\,T^j(x,t)\delta_S^j,
\end{aligned}$$

where, $J_I^{\pm}(x,t), i_0^{\pm}(x,t), \eta^{\pm}(x,t)$ are formulated by the following algebraic equations

$$\begin{aligned}
J_I^{\pm}(x,t) &= \frac{i_0^{\pm}(x,t)}{F}\left(e^{\frac{\alpha_n F\eta^{\pm}(x,t)}{RT^j(x,t)}} - e^{-\frac{\alpha_p F\eta^{\pm}(x,t)}{RT^j(x,t)}}\right),\\
i_0^{\pm}(x,t) &= k^{\pm}C_e(x,t)^{\alpha_n}(C_{\text{smax}}^{\pm} - C_{s,m}^{\pm}(x,t))^{\alpha_n}C_s^{\pm}(x,t)^{\alpha_p},\\
\eta^{\pm}(x,t) &= \Phi_s^{\pm}(x,t) - \Phi_e^{\pm}(x,t) - U^{\pm}(C_{ss}^{\pm}(x,t))\\
&\quad - FR_f(x,t_0)J_I^{\pm}(x,t)\,.
\end{aligned}$$

In this medium time scale battery model, the slow states, namely $C_{s,s}, Q_{sr}, R_f$, are all replaced by constants.

To individually investigate the behaviour of the slow state $\mathbf{x}_{s'}$ governed by (42), further model simplification is needed as the medium and slow time scales are still coupled through the input, $u(t)$, appearing. In the usual practice of singular perturbation approaches, the slow system is derived by approximating the fast dynamics with their quasi-steady state values. However, since charging and discharging represents a cyclical process the dynamics in the medium time scale do not approach a constant steady state, and this requires an alternative approach of analysis.

From *Assumption* 2, the system input $u(t)$ is known to be in the medium time scale for almost all time. Consideration of this and the smallness of $\frac{i_{0sr}}{i_o^*}$ imposed by *Assumption* 4 motivates the use of averaging theory [11], [12] to simplify the process of deriving the slow battery model with the state, $\mathbf{x}_{s'}$.

The solution of $\mathbf{x}_{s'}$ in the battery model (42) is obtained by averaging the steady-state behaviour of the medium battery system (43). Define a static, average mapping $\mathbf{x}_{s'}(t) \to \mathcal{H}_{av}(\mathbf{x}_{s'}(t))$ as:

$$\begin{aligned}
\mathcal{H}_{av}(\mathbf{x}_{s'}) := \lim_{T_s\to\infty}\frac{1}{T_s}\int_0^{T_s}&\mathcal{F}_m\mathbf{x}_m^*\\
&+ H_m(\mathbf{x}_{s'0},\mathbf{x}_m^*,h(\mathbf{x}_{s'0},\mathbf{x}_m^*,u^*),u^*)dt.
\end{aligned} \tag{44}$$

where $u^*(t)$ is the specified system input, $\mathbf{x}_m^*(t)$ is the solution of the battery model (43) under the specified system input $u^*(t)$. In this *general average* mapping, it is worth mentioning that $\mathcal{H}_{av}$ is independent of i_{0sr} and $(\mathbf{x}_m(0),u(0)) \in \mathscr{H}_m \times \mathbb{U}/\{0\}$.

Therefore, in the slow time scale $\sigma = \frac{i_{0sr}}{i_0^*}t$, the dynamics of $\mathbf{x}_{s'}$ from (42) are approximated by the following slow

(average) battery system, denoted Σ_s^3:

$$\frac{d\mathbf{x}_{s'}}{d\sigma} = \mathcal{H}_{av}(\mathbf{x}_{s'}),\ \mathbf{x}_{s'}(0) = \mathbf{x}_{s'0}, \tag{45}$$

$$\mathbf{y}_c = \mathcal{G}[\mathbf{x}_{s'}, \mathbf{x}_m^*, h(\mathbf{x}_{s'}, \mathbf{x}_m^*, u^*)]^T. \tag{46}$$

To enable averaging theory to be utilised in this manner for battery model simplification, an assumption is posed on the medium time scale dynamics. Define a manifold $\bar{\mathbf{x}}_m = h'(\mathbf{x}_{s'0}, u)$ representing the quasi-steady state of the medium state variables $\mathbf{x}_m$ of (43). Then $\bar{\mathbf{x}}_m$ is the solution of:

$$\dot{\bar{\mathbf{x}}}_m(t) = \mathcal{F}_m \bar{\mathbf{x}}_m(t) + H_m(\bar{\mathbf{x}}_m(t), u(t)), \tag{47}$$

where $u(t) = u(t + kT_c)$, $\forall k = 0, 1 \cdots N$.

Assumption 5: There exists an integral manifold $\mathbf{z}_m := \mathbf{x}_m - \bar{\mathbf{x}}_m$, where $\bar{\mathbf{x}}_m$ is defined in (47), and a class-$\mathcal{KL}$ function β_h such that, for all initial conditions in the domain $\mathcal{D}$, the solutions of $\mathbf{x}_m$ in Σ_m^3 exist and satisfy

$$|\mathbf{z}_m| \leq \beta_h(|\mathbf{z}_m(0)|, t), \forall t \geq 0. \tag{48}$$

The validity of Assumption 5 may be intuitively obvious for periodic inputs, as it states the medium time scale states will approach a periodic trajectory irrespective of their initial conditions at $t = 0$. The validity of this assumption can be quantitatively investigated via simulation.

If Assumption 5 is valid, only the behaviour of $\mathbf{x}_m$ governed by the battery system Σ_m^3 is required to find the developed mapping $\mathbf{x}_{s'} \to \mathcal{H}_{av}(\mathbf{x}_{s'})$. Once such a mapping $\mathcal{H}_{av}$ is obtained (and this can be done offline with *a priori* knowledge of the periodic input $u(t)$), the slow battery system becomes straightforward from (45)-(46).

To this point, PDE models of the battery dynamics have been established over three time scales using approaches based on singular perturbation theory from ordinary differential equations. The models Σ^1, Σ_f^2, Σ_s^2, Σ_m^3 and $\Sigma_{s'}^3$ serve as starting points for further model reduction depending on the characteristics required in the model and its subsequent use. In the following, it is assumed that state of charge estimation and control over relatively short durations is the principal objectives, and hence Σ_m^3 is considered as the base model for further reduction in the following sections. Note however, that the order of these further reductions, and indeed the base model they are applied to, is not unique.

IV. Model simplification through spatial dimension reduction

The model Σ_m^3 retains two spatial dimensions, x and r, and yet for state of charge estimation only the average concentration in the solid particles, $\bar{C}_s(x,t)$, and the surface concentration given in (6) are required. This motivates the removal of the r-dependence in the model.

The first step in this regard utilises an exact analytical solution of (13) provided by [13] as

$$C_s(x,r,t) = C_{s0} - \frac{J_I(x,t)\cdot R_P}{D_s}\left[3\tau + \frac{1}{10}\left(\frac{5r^2}{R_p^2} - 3\right)\right] + \frac{2J_I(x,t)\cdot R_P^2}{D_s r}\sum_{n=1}^{\infty}\frac{\sin(\lambda_n r/R_p)\exp\left(-\lambda_n^2\tau\right)}{\lambda_n^2\sin(\lambda_n)} \tag{49}$$

where, $\tau = D_s t/R_P^2$, and $\lambda_j (j$ = 1,2,...) are the positive eigenvalues of $\lambda_j = \tan(\lambda_j)$.

The infinite series of (49) motivates finding an approximation of C_s. An n-th order polynomial approximation was expressed in [14] as:

$$\hat{C}_{s,n}(x,r,t) = a_1(x,t) + a_2(x,t)\frac{r^2}{R_P^2} + \cdots + a_n(x,t)\frac{r^{2n}}{R_P^{2n}} \tag{50}$$

By substituting (50) into (13) and employing volume-average integration of r, the 2D second-order PDE in each electrode can be decoupled to a first-order PDE and an algebraic equation, $\bar{C}_s(x,t)$ and $C_{ss}(x,t)$:

$$\partial\bar{C}_s(x,t)/\partial t = -3J_I(x,t)/R_P \tag{51}$$

$$C_{ss}(x,t) = C_{s0} - \vartheta(x,t)(3\tau + 0.2) + \vartheta(x,t)\sum_{n=1}^{\infty}\frac{2\exp\left(-\lambda_n^2\tau\right)}{\lambda_n^2} \tag{52}$$

where for compactness $\vartheta(x,t) := J_I(x,t)R_P/D_s$. By choosing the second, fourth, and sixth-order polynomials for (50), equation (52) can be respectively represented as [14]:

$$C_{ss,1}(x,t) = C_{s0} - \vartheta(x,t)(3\tau + 0.2) \tag{53}$$

$$C_{ss,2}(x,t) = C_{s0} - \vartheta(x,t)\left(3\tau + 0.2 - 2e^{-35\tau}/35\right) \tag{54}$$

$$C_{ss,3}(x,t) = C_{s0} - \vartheta(x,t)\left(3\tau + 0.2 - 0.1135e^{-100.123\tau}\right) + \vartheta(x,t)\left(0.0864e^{-18.877\tau}\right) \tag{55}$$

Removal of the r-dimension from the Σ_m^3 model in this fashion leads to the reduced model denoted Σ_{r1}. The required order of the approximation n to attain a given level of accuracy is dependant on the variation of concentration in the spatial dimension, which in turn is affected by the magnitude of the input current, $u(t)$. This will be explored for different charging rates in the following section concurrently with other model reduction approaches.

V. Model simplification through Spatial Discretization

With a few notable exceptions, most controllers and estimators are designed around ODE representations of the system rather than PDEs. Here we explore the necessary dimensionality of lumped parameter approximations to the model, Σ_{r1}, arising from the previous section.

The PDEs in the reduced order model can be approximated by the well-established process of finite element approximation. This can be realized through discretizing each domain in the cell to N lumped elements with grid resolution Δx_i. In this way, by letting i denote the i-th element in each electrode or separator, a discretized battery model with uniform resolution is:

$$d\bar{C}_s(i)/dt = -3J_I(i)/R_P \tag{56}$$

$$C_{ss,n}(i): = C_s(i, R_p) \tag{57}$$

$$\mu_e\frac{dC_e(i)}{dt} = D_e\frac{C_e(i+1) - 2C_e(i) + C_e(i-1)}{(\Delta x)^2} + \gamma(i_e(i+1) - i_e(i))/(F\Delta x) \tag{58}$$

$$(\Phi_s(i+1)-\Phi_s(i))/\Delta x = -i_s(i)/\sigma(i) \quad (59)$$

$$(\Phi_e(i+1)-\Phi_e(i))/\Delta x = -i_e(i)/\kappa(i) + \frac{2RT(i)\gamma}{F}\frac{\ln C_e(i+1)-\ln C_e(i)}{\Delta x} \quad (60)$$

$$(i_e(i+1)-i_e(i))/\Delta x = aFJ(i) \quad (61)$$

$$J(i) = \frac{i_0(i)}{F}\left(e^{\frac{\alpha_a F\eta(i)}{RT(i)}} - e^{-\frac{\alpha_c F\eta(i)}{RT(i)}}\right) \quad (62)$$

$$\rho c\frac{dT(i)}{dt} = \lambda\frac{T(i+1)-2T(i)+T(i-1)}{(\Delta x)^2} + aFJ(i)(\eta(i)+T(i)\delta_S) - i_e(i)\frac{\Phi_e(i+1)-\Phi_e(i)}{\Delta x} - i_s(i)\frac{\Phi_s(i+1)-\Phi_s(i)}{\Delta x} \quad (63)$$

This reduced system, Σ_{r2} is a spatially discretized model that includes $8N$ ODEs and $11N$ algebraic equations associated with $19N$ states in the entire battery region. However, typical battery parameters like those observed in [15], [16] lead to separation of length scales between some states of Σ_{r2}.

To capture this effect, the $19N$ state equations will be considered with different level of discretization, particularly focusing on the temperature and electric potential states, which will have independent resolutions represented by N_T and N_Φ states respectively. This leads to $14N$+$2N_\Phi$+N_T total equations, with the size on each of the three variables dependant on the desired model accuracy (relative to the original system) and the applied charge rates.

These are now explored via numerical simulation to determine the minimum modelling requirements to maintain a predictive error capability in terminal voltage estimation of at most 1% RMS for a typical cell using constant currents in a range 0.5-10C. From Table I, it is apparent that a single lumped approximation for each of the states will result in good approximation of the Σ_m^2 system outputs at low charge rates. This particular model represents the well known *single particle model*, albeit with the presence of temperature and electrolyte states (the removal of which is a further model reduction as discussed in the following section).

Naturally, the requirement of 1%-accuracy in the terminal voltage estimation is somewhat arbitrary, and the use of the model in closed loop estimation and control applications may mean that feedback leads to higher degrees of error being tolerable while delivering satisfactory closed loop performance. What is appreciable however, is that for high current applications, the single particle model will not adequately capture the true model outputs well and higher degrees of resolution are required, as previously reported by [17].

Furthermore, while these tabulated results focus on the terminal voltage, the use of a reduced order model that is derived from Σ_m^3 is likely to focus on state of charge requirements. Consequently, the ability of the model to reproduce the relevant states of Σ_m^3 is illustrated in Figure 2 at low and high charge operation for the resolutions presented in Table I. It is evident that these internal states are also well captured.

TABLE I

MODEL REQUIREMENTS FOR 1% RMS ACCURACY OF MODEL OUTPUTS AT DIFFERENT CHARGE RATES.

Rate	n	N	N_T	N_Φ^-	% error
0.5C	1	1	1	1	0.39
1C	1	1	1	1	0.87
2C	1	3	1	1	0.73
3C	2	2	1	1	0.83
4C	2	5	1	1	0.94
5C	3	5	1	1	0.93
6C	3	6	1	1	0.99
7C	3	7	1	1	1.00
8C	3	8	1	1	0.96
9C	3	9	1	1	0.98
10C	3	10	1	1	0.99

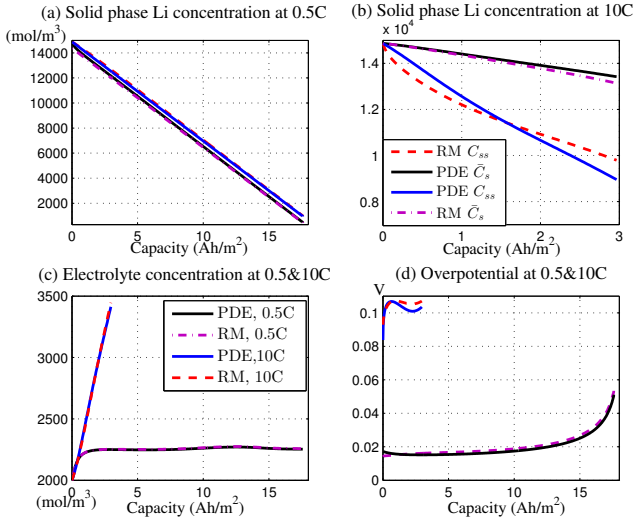

Fig. 2. Comparison of the reduced model (RM) and PDE model in terms of C_{ss}, $\bar{C}_s$, C_e, and η (at current collector) during 0.5C and 10C charge operations. For 0.5C, n=N=1; for 10C, n=3 and N=10.

VI. FURTHER MODEL SIMPLIFICATIONS

There exist further possibilities for model reduction based on elimination of states due to their insensitivity on the model output. If the starting point for further model reduction is considered to be Σ_{r2} operating at low currents (i.e. the single particle model with both temperature and electrolyte contained).

Assumption 6: The temperature at the surface of the cell is measurable.

As only a single temperature state is required even at high input currents, measurement of the current anywhere on the cell is likely to lead to a reasonable approximation of the internal lumped state. Use of this assumption, and the subsequent removal of the temperature states leads to a single particle model with liquid diffusion.

Assumption 7: The net flow of ions between the electrolyte and the solid particles is sufficiently small for all time.

This allows a conservation equation to be used to solve for the electrolyte concentrations, and their states can be

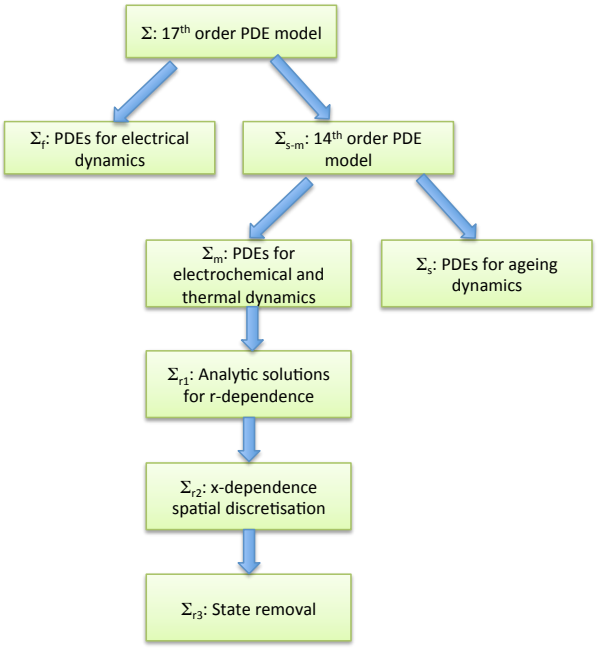

Fig. 3. Simplification steps in generating single particle model

removed form the model. There is motivation to remove the electrolyte equations following this assumption, rather than the solid particles as all output calculations are stated in terms of the latter states. This assumption leads to the single particle model representation without either liquid diffusion or thermal states.

The full process of model simplification starting from the full order model Σ_1 is illustrated in Figure 3.

VII. Conclusions

Model simplification and reduction procedures based around time and length scale separation have been used to derive the single particle model from the original PDE-based battery model. The steps highlighted can be used in different ways to generate alternative models depending on the estimation and control requirements of a given application (for example, ageing dynamics may be maintained if state of health is a part of the problem solution). The approaches have been demonstrated on one particular version of the battery model, but can be utilised by other models if more accurate models become available (for example the ageing process has no universally accepted dynamic model at this stage).

References

[1] N. A. Chaturvedi, R. Klein, J. Christensen, J. Ahmed, and A. Kojic, "Algorithms for advanced battery-management systems," *IEEE Trans. Control Syst. Mag.*, vol. 30, no. 3, pp. 49–68, Jun. 2010.

[2] P. Ramadass, B. Haran, P. M. Gomadam, R. White, and B. N. Popov, "Development of first principles capacity fade model for Li-ion cells," *J. Electrochemical Society*, vol. 151, no. 2, pp. A196–A203, 2004.

[3] G. Ning, R. E. White, and B. N. Popov, "A generalized cycle life model of rechargeable Li-ion batteries," *Electrochimica Acta*, vol. 51, no. 10, pp. 2012–2022, 2006.

[4] M. Doyle, T. F. Fuller, and J. Newman, "Modeling of galvanostatic charge and discharge of the lithium/polymer/insertion cell," *Journal of The Electrochemical Society*, vol. 140, no. 6, pp. 1526–1533, 1993.

[5] W. B. Gu and C. Y. Wang, "Thermal-electrochemical modeling of battery systems," *J. Electrochemical Society*, vol. 147, no. 8, pp. 2910–2922, 2000.

[6] J. Newman and K. E. Thomas-Alyea, *Electrochemical systems*. John Wiley & Sons Inc., 2012.

[7] A. Barre, B. Deguilhem, S. Grolleau, M. Gerard, F. Suard, and D. Riu, "A review on lithium-ion battery ageing mechanisms and estimations for automotive applications," *J. Power Sources*, vol. 241, pp. 680–689, 2013.

[8] P. D. Christofides, *Nonlinear and robust control of PDE systems: Methods and applications to transport-reaction processes*. Springer, 2001.

[9] P. V. Kokotovic, R. O'malley, and P. Sannuti, "Singular perturbations and order reduction in control theory–an overview," *Automatica*, vol. 12, no. 2, pp. 123–132, 1976.

[10] H. K. Khalil, *Nonlinear systems*. Prentice hall Upper Saddle River, 2002, vol. 3.

[11] P. Kokotovic, H. K. Khalil, and J. O'reilly, *Singular perturbation methods in control: analysis and design*. Siam, 1999, vol. 25.

[12] A. R. Teel, L. Moreau, and D. Nesic, "A unified framework for input-to-state stability in systems with two time scales," *IEEE Trans. Automatic Control*, vol. 48, no. 9, pp. 1526–1544, 2003.

[13] H. Carslaw and J. Jaeger, *Conduction of Heat in Solids*. London: Oxford University Press, 1973.

[14] V. R. Subramanian, J. A. Ritter, and R. E. White, "Approximate solutions for galvanostatic discharge of spherical particles i. constant diffusion coefficient," *J. Electrochemical Society*, vol. 148, no. 11, pp. E444–E449, 2001.

[15] M. Doyle, J. Newman, A. S. Gozdz, C. N. Schmutz, and J.-M. Tarascon, "Comparison of modeling predictions with experimental data from plastic lithium ion cells," *J. Electrochemical Society*, vol. 143, no. 6, pp. 1890–1903, 1996.

[16] W. B. Gu and C. Y. Wang, "Thermal and electrochemical coupled modeling of a lithium-ion cell," *Proc. Electrochemical. Soc.*, vol. 99, pp. 748–762, 2000.

[17] S. Santhanagopalan, Q. Guo, P. Ramadass, and R. E. White, "Review of models for predicting the cycling performance of lithium ion batteries," *J. Power Sources*, vol. 156, no. 2, pp. 620–628, 2006.